



## Full Length Article



# Experimental and numerical investigation of mercury removal from flue gas by sorbent polymer composite

Arkadiusz Ryfa<sup>a,\*</sup>, Robert Żmuda<sup>b</sup>, Sergiusz Mandrela<sup>b</sup>, Ryszard Białecki<sup>a</sup>,  
Wojciech Adamczyk<sup>a</sup>, Marcin Nowak<sup>e</sup>, Łukasz Lelek<sup>b</sup>, Dominika Bandoła<sup>a</sup>, Marcin Pichura<sup>b</sup>,  
Joanna Płonka<sup>c</sup>, Magdalena Wdowin<sup>d</sup>

<sup>a</sup> Department of Thermal Engineering, Silesian University of Technology, Konarskiego 22, 44-100 Gliwice, Poland

<sup>b</sup> SBB Energy S.A., ul. Lowicka 1, 45-324 Opole, Poland

<sup>c</sup> Department of Inorganic Chemistry, Analytical Chemistry and Electrochemistry, Silesian University of Technology, Krzywoustego 6, 44-100 Gliwice, Poland

<sup>d</sup> Mineral and Energy Economy Research Institute of the Polish Academy of Sciences ul. J. Wybickiego 7A, 31-261 Kraków, Poland

<sup>e</sup> AGH University of Science and Technology, Faculty of Metals Engineering and Industrial Computer Science, Department of Applied Computer Science and Modelling, Poland

## ARTICLE INFO

## Keywords:

Sorbent polymer composite  
Mercury emission reduction  
Energy sector  
Air pollution control  
Power plants  
CFD  
Numerical model

## ABSTRACT

This paper presents an experimental and numerical investigation of the performance of a sorbent polymer composite (SPC) material used for removing mercury from the flue gases in a full-scale industrial installation. The investigated material is an attractive alternative to activated carbon, which is commonly used for this purpose. While the application of the SPC is characterized by high capital expenditures, this technology offers not only very low operating expenditures but also high efficiency. This study investigates the SPC's mercury reduction capabilities concerning the most important flow parameters such as gas velocity, temperature, humidity, and mercury concentration. Small scale laboratory experiment was used to tune the kinetic data of the mercury adsorption. The resulting sub-model has been built into the CFD simulations validated against measurements at an industrial installation. The results showed that the most important parameters affecting the mercury reduction efficiency were the gas velocity and mercury content in the sorbent material. Numerical simulation proved that the material absorbs mercury within the entire reasonable operating temperature and humidity ranges, regardless of mercury speciation.

## 1. Introduction

Mercury (Hg) is a metal that can be found in the natural environment, and small amounts are found in fossil minerals, most often in the form of mercury sulfide (HgS). The largest anthropogenic source of mercury emissions in Europe and the second largest in the World is the combustion of fossil fuels, with mercury released in an elemental form Hg<sup>0</sup> [5]. When the metal vapor contacts halogens (chlorides, bromides, fluorine) it is partially converted into oxidized mercury Hg<sup>2+</sup> and partly adsorbed by fly ash [27]. Mercury is present also in waste gases from other industrial processes. According to the World Health Organization (WHO) [25], contact with even a small amount of mercury in the air, water, or soil causes serious threats to life and health. WHO includes mercury among the ten most dangerous toxic chemicals. Mercury poisoning has dangerous social consequences and affects the state of the

environment. It is accumulated in living organisms (people, animals, and plants) throughout their lives, which makes the treatment of mercury poisoning extremely difficult. Thus, the only reasonable policy to prevent this medical condition is to reduce mercury emissions into the environment [4].

The acceptable mercury concentrations released from power plants depend on the type of fuel being burned and are defined at different levels by several countries. According to the directive of the European Parliament [2], the admissible mercury emission from power units of power > 300 MWt is 1–2 µg/Nm<sup>3</sup> for hard coal and 7 µg/Nm<sup>3</sup> for lignite. Further tightening of emission standards to 1 µg/Nm<sup>3</sup> is foreseen. In the USA, the permissible emissions are currently 1.7 µg/Nm<sup>3</sup> and 15.3 µg/Nm<sup>3</sup>, respectively [11]. Soon, these standards will be greatly reduced to about 0.03 µg/Nm<sup>3</sup> for hard coal and 5 µg/Nm<sup>3</sup> for lignite [21].

Some level of reduction can be achieved by tuning the existing

\* Corresponding author at: Konarskiego 22/104, Department of Thermal Engineering at Silesian University of Technology, 44-100 Gliwice, Poland.  
E-mail address: [Arkadiusz.Ryfa@polsl.pl](mailto:Arkadiusz.Ryfa@polsl.pl) (A. Ryfa).

installations, such as denitrification [26] (oxidation of mercury from  $Hg^0$  to  $Hg^{2+}$ ), electrostatic precipitators (ESP) [10], baghouse filters (capture of fly ash containing Hg), or wet flue gas desulphurization (FGD) installations (removal of oxidized mercury with wastewater) [8,14,19]. One has to keep in mind that mercury present in captured dust can also pose a threat for further use of such dust [20]. Such measures may be sufficient for current emission standards and installations fired with bituminous coal, but they are not sufficient for those that use lignite. To meet the increasingly stringent mercury emission standards, additional measures should be implemented. The available methods include the addition of fuel additives and the injection of mercury scavengers, such as activated carbon, into the exhaust gases. Tightening emission standards and raising public awareness is a motivation to introduce other innovative technologies for mercury capture.

Many literature studies have reported the injection of additives to the flue gas downstream of the boiler. The most common additive is activated carbon [15,22,28,31], which can be injected either in its pure or modified forms. Modification of activated carbon is usually achieved by impregnating it with bromides, sulfides, or chlorides [33,1,16,17,32]. The practical implementation of carbon injection is the use of finely powdered activated carbon into the flowing exhaust gas, upstream of the electrostatic precipitator [27]. The injected carbon adsorbs both elemental and oxidized mercury [27]. Mercury adsorbed on the surface of activated carbon is then removed in the electrostatic precipitator as Hg-bound mercury [15]. The most important parameters affecting the efficiency of mercury removal by activated carbon are the granulation and porosity of coal and its distribution in gas. Such an approach has numerous advantages, the most important being the possibility of adjusting the amount of injected carbon to the current concentration of mercury in the flue gases and low capital expenditures (CAPEX). On the other hand, the technology requires large amounts of carbon, which not only raises operating expenditures (OPEX) but also increases the carbon content in the captured ash, which reduces its commercial value. There are studies that deal with the effect of flue gas temperature influence on activated carbon performance [30]. Other additives [23,9,18,3] can be injected, such as calcium sorbents, petroleum coke, zeolites, and fly ash, but brominated activated carbon is currently the most used medium [29]. Recently there have been studies where more complex additives were analyzed. Liu [13] analyzed a composite adsorbent (CuS/MWCNTs) that binds mercury to HgS, Wei [24] considered application of intercalated K for capturing mercury from flue gas.

Numerical simulation is one of the tools that allows for reduction the prototyping time and cost. It can be used to predict the behavior of the system for off design conditions. Computational fluid dynamics (CFD) can be used to test the performance of various methods for mercury reduction. CFD was used to foresee the mercury capture from flue gases by zeolites (Janchen 2015) where fixed bed of honeycomb shape was analyzed. A mathematical model for mercury capture by the injection of the activated carbon into the gas duct has been developed in (Zhou 2015). A CFD simulation of an electrostatic precipitator was carried out to determine the effectiveness of combined dust and mercury removal (Feng 2020), [12].

This paper investigates the crucial features of a novel mercury removal technology where mercury is adsorbed by a sorbent built in a polymer membrane (sorbent polymer composite – SPC). Since this material is rather new to the market, there is no comprehensive study of its reduction capabilities. Some information on this mercury control technique can be found in refs [7,6]. SPC is a solid material in the form of thin sheets mounted in the flue gas channel at the top of a wet flue gas desulphurization (FGD) unit or further downstream in the flue gas duct. Compared with its counterparts i.e., carbon injection, the use of SPC requires significant modification of the wet scrubber or flue gas duct, which leads to increased CAPEX. On the other hand, only periodic washing is required during SPC operation, which results in very low OPEX. Additionally, mercury is permanently chemically bound within

SPC which, after the lifespan of SPC has passed (about 10 years), minimizes the costs of final disposal of the used membranes.

This paper analyzes the performance of an SPC material in a laboratory and a full-scale experiment under typical operating conditions. Tests are aimed at determining how long SPC materials can maintain their capturing properties. Therefore, the tested material was preloaded with mercury to simulate long-term operation under real conditions. A numerical model of a large-scale installation was developed and validated against experimental data.

## 2. Experimental setup

For the development of the numerical model, two experimental setups have been developed. First was a laboratory scale rig devoted to testing the long-time performance of the SPC material. The second was an industrial-scale rig that was used to test the performance of clean material under real conditions.

The tested material is a composite produced by GORE [6]. The microscopic structure of the sorbent polymer composite (SPC) material is schematically shown in Fig. 1. The SPC material is a unique porous composite membrane based on the combination of active particles made mostly of activated carbon with small amount of polytetrafluoroethylene (PTFE).

The activated carbon particles are securely held within the membrane by PTFE fibers, represented by the lines shown in Fig. 1. The active particles have multiple functions. They are designed to chemically react with mercury molecules in the flue gas, forming stable solid mercury compounds that remain in the system and are thereby removed from the flue gas. These are then adsorbed onto the internal carbon surfaces, where they remain in the system and mercury is therefore removed from the flue gas. The sorbent present in SPC material efficiently captures both elemental and oxidized mercury and is insensitive to fuel or process changes. In addition, the active particles are designed to be catalytically active toward  $SO_2$  oxidation.  $SO_2$  molecules are adsorbed onto the activated carbon particles together with oxygen and water molecules, where they are catalytically converted into  $H_2SO_4$ . When the sulfuric acid penetrates the hydrophobic capillaries in the PTFE microporous matrix, it is not stable and will be expelled to the SPC external surfaces, thereby securing continued gas access to the active particles. The presented material does not require additional sorbents or chemicals to be injected. Also, there is no concern over fly ash contamination, halogen-induced corrosion, or wastewater treatment complications [6].

The polymer material is made in a form of flat and wavy sheets which are then packed in boxes (modules) and stacked/arranged inside a gas duct. The number of layers depends on the desired mercury reduction level. The operation of such a system is very simple as it requires only

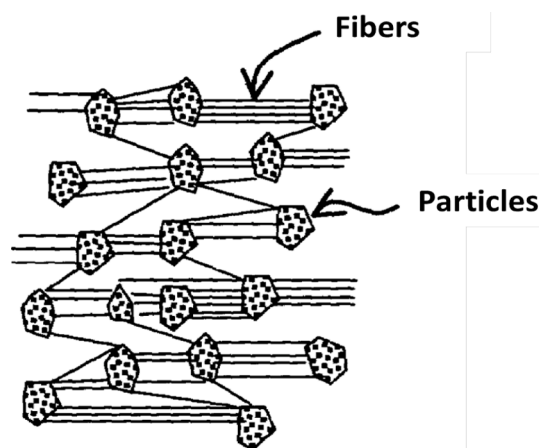


Fig. 1. Schematic representation of the Sorbent Polymer Composite (SPC) material.

washing with water twice a day to remove any attached dust and to wash off sulfuric acid. The designed operation time of a such system is 7 to 10 years with one possible reversing layer of modules in the middle of the operation procedure. As the mercury is permanently bound within a polymer structure there is no problem with mercury re-emissions from a wet flue gas desulfurizationsystem, eliminating the need for re-emissions additives. After the exploitation period is over, the material is removed from the structure frame and has to be stored as a dangerous waste. One has to keep in mind that the volume of the material to be stored is small in comparison to the volume of injected sorbents resulting in lower disposal costs. It is nothing special in the material itself, consisting of a polymer PTFE matrix in which particles of activated carbon are immobilized. In the alternative, widely applied technology, the same carbon is injected to the combustion gases to remove mercury. By keeping the carbon in the properly shaped foil, the time and surface of contact of the active component with the flue gases can be controlled. Thus, the mercury is not transferred to the ash (spoilng its quality and commercial value) but are accumulated in a safe manner within the plant. Disposal of the film takes place after a long period of time (about 10 years) and is a well-controlled process.

### 2.1. Laboratory experiments

As already mentioned he expected lifetime of an SPC material for power plant applications is about 7 to 10 years. During this period, the membranes undergo mechanical wear, and their capture potential is reduced due to the already adsorbed mercury. The wear is difficult to simulate because of the long time and dependence on fly ash content and quality. Thus, the investigation of mechanical wear is out of the scope of this paper. The admissible operation time of a membrane also depends on the mercury concentration in the flue gas, the desired reduction level, gas velocity, and humidity. Conducting 10 years of measurements is not feasible. To take the accumulation of mercury in the membranes the samples were preloaded with mercury. The preloading of SPC samples was performed in a sealed chamber located in a fume hood. There, samples were mounted above a liquid metallic mercury surface. To speed up the preloading procedure, the entire chamber was heated in a water bath to 338 K. The aim was to get samples with various mercury concentrations and to find the maximum mercury concentration in SPC material. Due to strong and rapid moisture absorption from the air mercury content could not be determined by weight. Thus, X-ray fluorescence (XRF) was used to measure mercury content in the preloaded

SPC membrane.

Once the samples were preloaded with mercury, they were used in the test rig whose aim was to investigate the adsorption process. After the tests, the sample was ground in a cryogenic mill, and the obtained powder was used to prepare a pill that was to be used in the X-ray Fluorescence spectrometer (XRF) yielding the actual mercury concentration in the SPC. First tests were conducted to determine the loading curve. The results showed that within the investigated load limits, the concentration of mercury increases linearly in time. The second observation concerned the maximum mercury concentration, which was about 15 wt%. For the expected 10 years of operation for typical power plant conditions and the desired mercury concentration, the total load should not exceed 4 wt%. To be on the safe side, however, concentrations between 0 and 10 % were used in this study.

The test rig, schematically shown in Fig. 2, consisted of four main parts: gas preparation unit, controlling section, measurement chamber, and mercury measurement section. The gas preparation unit used a HovaCAL digital MF 411 (MG) to prepare gas containing the desired mercury content.

The operating principle of this device was to mix the carrying gas (primary air) with evaporated water solution of  $\text{HgCl}_2$  stabilized by HCl. Next, air containing mercury was mixed with ambient air – secondary air, to obtain the final desired mercury concentration. The controlling section is responsible for maintaining the temperature, flow, and humidity of the gas. The flow of secondary air was controlled by a Bronkhorst F-111AC (FC, uncertainty 0.5 %) and HovaCAL MF (uncertainty 2 %) for the air and mercury mixture. The volume  $0.4\text{--}2\text{ Nm}^3/\text{h}$  of secondary air is delivered through compressor C and pressure controllers PC1 and PC2. Humidity was measured using an EE160HT6XXPBB probe (uncertainty of 2 % at 25 °C) mounted near the inlet of the measurement chamber (T5). Water mist was dosed to the gas using an ultrasonic spraying system AccuJet (S), which generated a very fine water mist that evaporated in contact with hot air. The water flow ( $\text{H}_2\text{O}$ ) was controlled via a peristaltic pump (uncertainty 0.001 g/s). The temperature of gas was controlled by three electric heaters equipped with type-T thermocouples (uncertainty 0.2 K). The first one H1 was mounted in the high-concentration mercury duct. It heated up gas outflowing from MG from T2 (180 °C). This heater gave the possibility to heat the gas up to 1073 K (T3). When heated to this temperature, the oxidized mercury is converted to metallic mercury. This conversion is important for speciation tests, where the sensitivity of the adsorption to the ratio of metallic and oxidized mercury was investigated.

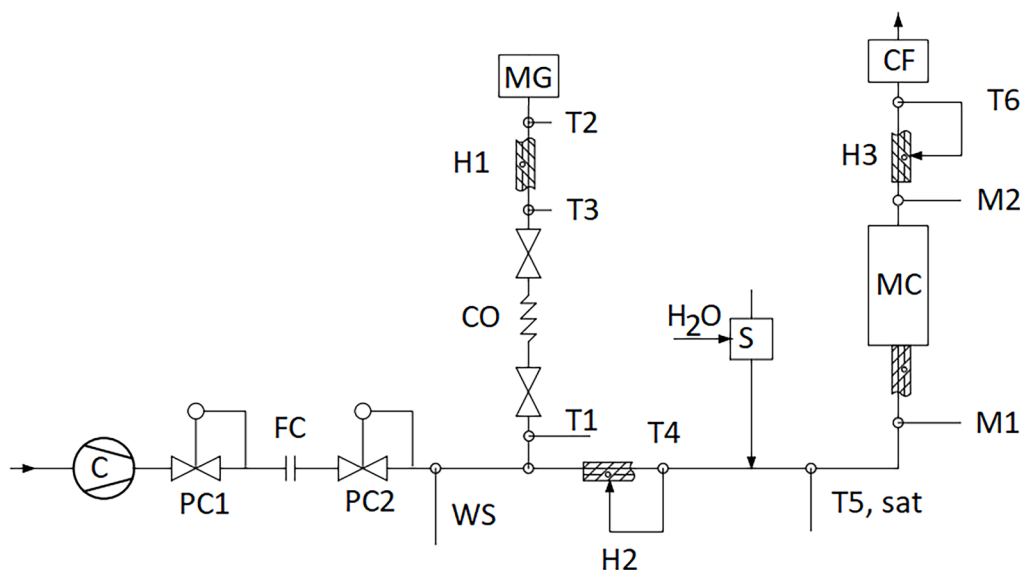


Fig. 2. Laboratory scale test rig.

Downstream to the heater *H1* a cooler (*CO*) is located. There the gas is cooled to 30–300 °C. Lower temperature is achieved when *H1* is disabled and higher for maximum temperature *T3*. Cooling is important and its main task is to prevent a mixed gas being too hot for heater *H2*. The second heater *H2* was mounted before the spraying system and was used to set the desired temperature in the measurement chamber (*MC*). The last heater *H3* was mounted behind the measurement chamber to increase the temperature before the active carbon filter. Its purpose was to heat up gas leaving the rig to about 90–100 °C (*T6*) which allows to avoid (or at least reduce) the condensation of water inside the filter. The active carbon (*CF*) filter was mounted at the outlet of the installation to remove any mercury emissions into the ambient atmosphere.

The measurement chamber (*MC*) assembly consists of the chamber itself and two mercury sampling ports located at the inlet (*M1*) and outlet (*M2*) of the chamber. The measurement chamber is a simple rectangular duct with a cross-section of 20x15 mm and a height of 300 mm. The chamber was designed to accommodate two flat and one wavy SPC modules. They are mounted to reproduce the configuration of membranes used in full-scale real systems. The latter contains dozens of modules that form many ducts. As it is very difficult to reproduce the real channel geometry or to use the entire package with SPC material in the experiments, it was decided to use only a small portion of the material. The rig contains two ducts as in actual applications (see A in Fig. 3) and two halves of ducts (see B in Fig. 3).

In such a configuration, the ratio of the SPC active perimeter per channel cross-section area was 1.63-times higher than in industrial applications. To account for this, a correction factor was introduced. The differential mass balance at a given cross-section of the channel assuming linear kinetics of the adsorption reads.

$$A_{ch}v dC = -kC dL \quad (1)$$

where  $A_{ch}$  is channel cross-section (m<sup>2</sup>),  $v$  is the gas velocity (m/s),  $C$  is mercury concentration (μg/Nm<sup>3</sup>),  $k$  is the overall transport coefficient (m/s), and  $L$  is the length of a channel. Solving Eq. (1) for the concentration profile of entire channel length  $L$  results in,

$$C_{out} = C_{in} e^{-\left(\frac{P_{SPC}L}{vA_{ch}}\right)} \quad (2)$$

Where  $C_{in}$  is the mercury concentration at the inlet to the channel,  $C_{out}$  is the concentration at the channel outlet, and  $P_{SPC}$  is the SPC material perimeter in contact with the flowing gas. Introducing the formula for mercury reduction given as.

$$\varepsilon_{Hg} = \frac{C_{in} - C_{out}}{C_{in}} \quad (3)$$

into equation (2) allows the reduction to be expressed as a function of SPC surface area. Assuming that the overall transport coefficient does not change allows for scaling the mercury reduction between different SPC module packing in the channel. Assuming constant  $k$  is justified as measurements were conducted at the same flow parameters as in real operation. Solving equation (2) for  $k$  and substituting  $\varepsilon_{Hg}$  gives.

$$k = -\frac{A_{ch}}{P_{SPC}} [v \ln(1 - \varepsilon_{Hg})] \quad (4)$$

Therefore, for the same velocity  $v$ , length of the channel  $L$  and transport coefficient  $k$ , the reduction depends only on the ratio of the channel area to the SPC perimeter. So, using the condition for equal  $k$ .

$$-\frac{A_{ch}}{P_{SPC}} [v \ln(1 - \varepsilon_{Hg})] = -\frac{A_{ch}^*}{P_{SPC}^*} [v \ln(1 - \varepsilon_{Hg}^*)] \quad (5)$$

reduction obtained in laboratory conditions  $\varepsilon_{Hg}$  can be scaled to the actual geometry of the full-scale (industrial) system  $\varepsilon_{Hg}^*$  obtaining.

$$\varepsilon_{Hg}^* = 1 - (1 - \varepsilon_{Hg})^{\frac{A_{ch}}{P_{SPC}} \frac{P_{SPC}^*}{A_{ch}^*}} \quad (6)$$

As mentioned for the case at hand, the active SPC area is higher, and we finally obtain.

$$\varepsilon_{Hg}^* = 1 - (1 - \varepsilon_{Hg})^{1/1.63} \quad (7)$$

## 2.2. Industrial scale experiment

The aim of the industrial-scale experiment was to test the performance of full SPC modules in contact with actual flue gas. Thus, a rig equipped with a fan and column where SPC modules are located was mounted on the flue gas bypass in lignite-fired power plant. The test rig, shown in Fig. 4, use flue gas taken from a duct before FGD and consists of a measurement chamber where 6 SPC modules are stacked, measurement ports, temperature, pressure and flow meters, water spraying system and a fan that is used to regulate the flow through a rig.

The exhaust fan sucks from a flue gas duct from 5000 to 5500 Nm<sup>3</sup>/h of flue gas, which was then directed to the absorption column containing 6 polymer modules arranged in series (vertically). Before and after the collector, the pressure and temperature of the exhaust gases were continuously measured. A venturi was installed downstream of the fan to verify the flue gas flow. In addition, the installation was equipped with a sprinkler system, including a water tank and a sewage tank with a visor and a drainage system. This system operated automatically in a sequential manner. The flue gas ducts, collectors, and the wash water system have been properly insulated to limit heat loss. The pilot installation was also equipped with the necessary devices ensuring safe and stable operation and a GSM module allowing for a remote change of settings and process visualization. Before taking the actual mercury measurements, the installation was subjected to a conditioning process, i.e. continuous operation for two months to saturate its components with mercury.

The mercury concentration is measured continuously by the Gasetm CMM system. It is designed for monitoring total mercury (i.e. atomic Hg<sup>0</sup> and oxidized Hg<sup>2+</sup>, HgCl<sub>2</sub>) based on the principle of spectroscopy of Cold Vapor Atomic Fluorescence (CVAF). The integrated high-temperature dry thermal converter turns all mercury compounds into atomic mercury. This way any problems associated with the re-production of mercury compounds during the transport of the gas can be eliminated. The Gasetm CMM consists of: the sampling device (heated probe made of high-alloy stainless steel coated internally with quartz glass, a sample suction system with a particulate filter, and a four-wire heated hose with internal wiring made of PFA Teflon); CVAF spectrophotometer with built-in high-temperature converter (atomizer); calibrator generating standard gas with any mercury content in the range from 0 ÷ 100 μg/m<sup>3</sup> which allows for checking and calibrating the CVAF spectrophotometer to the required range. Apart from mercury also sulfur dioxide, carbon mono, dioxide, oxygen, and NO<sub>x</sub> were measured.

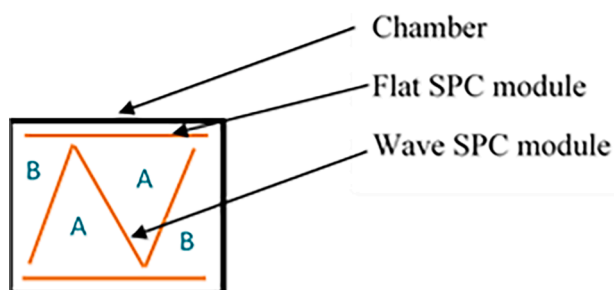


Fig. 3. Cross-section of the measurement chamber.





Fig. 4. Industrial scale test rig: scheme (left) and photo (right). In the photo: 1 – SPC modules, 2 – mercury measurement (GASMET), 3 – fan, 4 – Venturi, 5 – flue gas bypass, 6 – water tank, 7 – water spraying system.

### 3. Measurement results

#### 3.1. Laboratory experiment

Gas containing mercury at the inlet and outlet of the chamber is heated to prevent temperature reduction leading to improper sensor readings. To gather data on the mercury concentration at these two locations, two Nippon Instruments mercury analyzers, EMP-3 with SGM-8, were used. The accuracy of the measurements at mercury concentrations from 10 to 100  $\mu\text{g}/\text{Nm}^3$  was  $\pm 0.1 \mu\text{g}/\text{Nm}^3$ . Each set measured either the total mercury or elemental mercury concentration, depending on the chemical compounds used. The device calibrated itself every 15 min, and data were logged with a time resolution of 1 s. Chemical compounds feeding the devices were automatically replaced every 2 h. Since both Nippon devices started the measurements at the same time, the compound replacement was also synchronized, which is important because the replacement process of the chemicals in the sensors can disturb the measurements. Before the actual measurements, the rig was conditioned with a gas containing mercury and without any tested material inside.

The measurement procedure is as follows. First, initial stoichiometric and thermodynamic calculations were performed to determine the ratio of primary to secondary air, the mercury content in primary air, and

heater settings. Next, the rig was turned on, and the gas began to flow. When constant parameters (gas velocity, temperature, humidity, and mercury concentration) were reached, the SPC module was mounted on the rig, and the mercury content was logged. Then, the mercury reduction was computed using equations (3) and (7).

The measurement of the mercury concentration in the channel versus time is given in Fig. 5, where regular peaks in both measured values are visible. They are the result of the flushing of the Nippon mercury analyzer and the chemical compound replacement.

Except for these peaks, the readings were stable. After an initial period of stabilization of the readings, the concentration of mercury at the inlet reached a steady state. As can be seen both inlet and outlet readings, exhibit oscillation which is a feature of the measuring device. These oscillations result from a high sampling rate and very small mercury concentrations. For this reason, sensor readings were averaged over time, and a single value was taken to calculate the mercury reduction. However, there were three different periods of the readings at the outlet. The first, (A), does not correspond to real measurement but represents the initial period (when analyzers are starting). The next two (B) and (C) are two measurements of different SPC samples. To calculate the average inlet/outlet mercury concentration, an average value was taken from the time between the peaks (red solid/dash and green solid/

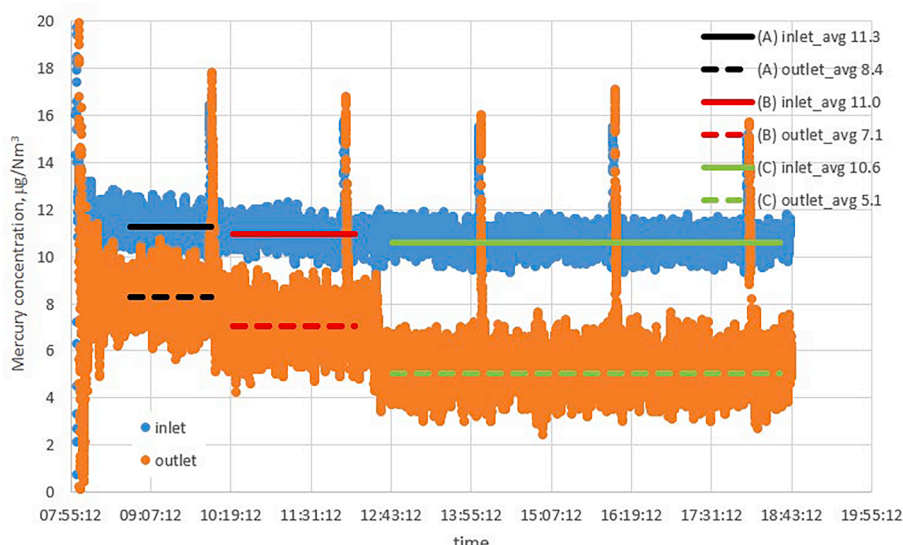


Fig. 5. The measurement data were collected for an entire day.

dash lines).

First laboratory tests were carried out on samples that did not contain mercury. Tests were run using typical industrial parameters i.e. gas velocity of 4 m/s, temperature of 338 K, 100 % humidity (full condensation that occurs after the wet scrubber), and an inlet concentration of mercury of  $12 \mu\text{g}/\text{Nm}^3$ . The performance was tested for metallic and oxidized mercury as well as dry and wet gas. Fig. 6 shows the mercury reduction under various conditions, which show that neither the mercury oxidation level (speciation) nor the humidity influence the mercury adsorption for membranes not preloaded with mercury.

The measured reduction ranged from 32 to 37 %, with only one result lower than 30 %. Measurement no. 1 differs significantly from the others. The differences can be explained by the local inhomogeneity of the material. In the case of industrial applications, the large amount of SPC makes such material inhomogeneity negligible. The average value of the reduction computed from all results was 34 %. The finding that humidity does not affect the results is an important result. The membrane is hydrophobic, and moisture condenses on its surface, partially blocking contact between the SPC surface and the gas. This, however, does not appear to influence the ability of the membrane to adsorb mercury. As working with condensed water is much more troublesome than in the case of dry gas, further tests were carried out using dry gas and oxidized mercury. The only humidity came from the ambient air, which resulted in a relative humidity of 8–10 % in the measurement chamber. Next tests were performed to examine the influence of temperature on the SPC performance (see Fig. 7). These temperatures were selected to match typical wet scrubber operating temperatures. One must bear in mind that the maximum continuous operating temperature of the SPC material is 353 K. The results show that there is only a slight decrease in the reduction upon increasing the temperature.

The next analyzed parameter was the inlet mercury concentration, which is important during the standard operation of a power plant, as the mercury concentration in flue gas can vary greatly. Five tests for inlet concentrations ranging between 10 and  $100 \mu\text{g}/\text{Nm}^3$  were conducted. Those test results ranged from 31 to 34 %, so the span is close to the initial tests. The results proved that the inlet mercury concentration did not affect the reduction ability of the SPC material. Furthermore, when the mercury concentration in the gas rapidly increased, the tested sample showed no delay in reduction. More importantly, a 30 % reduction at  $100 \mu\text{g}/\text{Nm}^3$  means a much greater mercury amount was adsorbed than at  $10 \mu\text{g}/\text{Nm}^3$ . These features have two important practical implications. First, the risk of sudden large mercury emissions is low, and second, it is better to use the SPC material as the first stage of

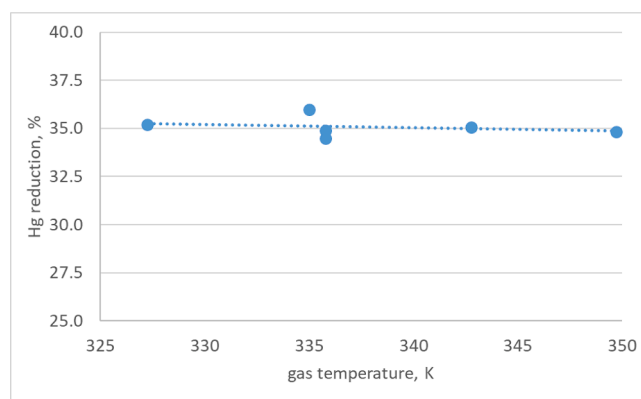


Fig. 7. Mercury reduction as a function of inlet gas temperature for non-preloaded samples.

reduction because it reduces the concentration by a given percentage, allowing additional methods (like activated carbon) to further tune the reduction downstream.

In the next step, the preloaded samples were used to test the influence of SPC mercury content on the reduction ability of the membrane. The results are shown in Fig. 8. Any amount of mercury preloaded in the SPC material deteriorates mercury adsorption. There is a sudden and significant drop in the SPC performance, even for the smallest mercury concentration of 0.14 %. This means that, even after a short time, the performance of SPC material is greatly reduced. The reduction of the pre-loaded sample is about 24 %, while the non-preloaded material reduced the mercury concentration by about 34 %. When the mercury loading was around 2 wt%, the mercury reduction in the gas further decreased to about 17 %. Such behavior is due to adsorption. Namely, mercury adsorption from gas occurred at the active centers in the SPC material. As more active centers were occupied by mercury molecules, the probability of capturing additional mercury molecules from the gas decreased. Thus, as expected, the mercury reduction decreased upon increasing the material's mercury content. This has to be taken into consideration when designing an industrial system. When the mercury concentration in SPC material exceeds 4 % the mercury concentration downstream is higher than upstream (yellow points in Fig. 8). This is especially visible for three measurement points in the vicinity of 4 %wt of mercury in the tested material. There one measurement showed reduction larger than expected i.e. at the level of 18 %, second reduction was at the level of 5 % which is less than expected. The third

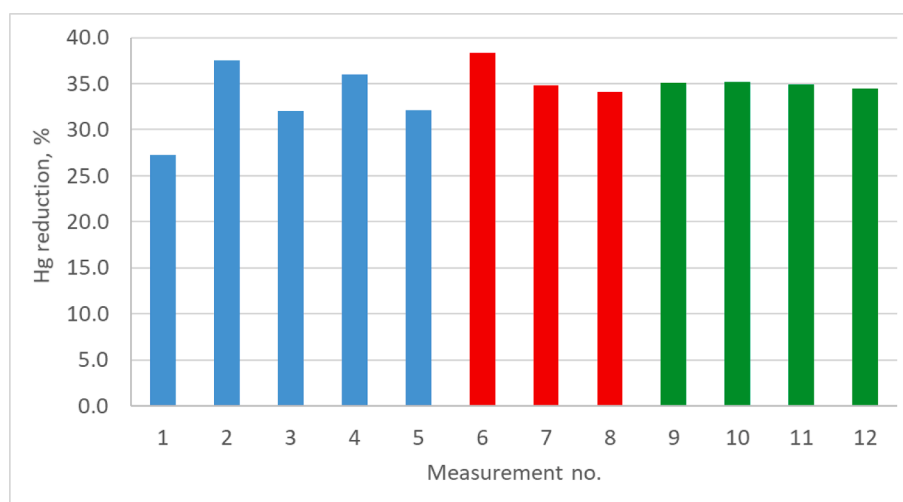


Fig. 6. Mercury reduction of samples without preloaded mercury (blue – dry, oxidized mercury, green – dry, metallic mercury, red – wet, metallic mercury). (For interpretation of the references to colour in this figure legend, the reader is referred to the web version of this article.)

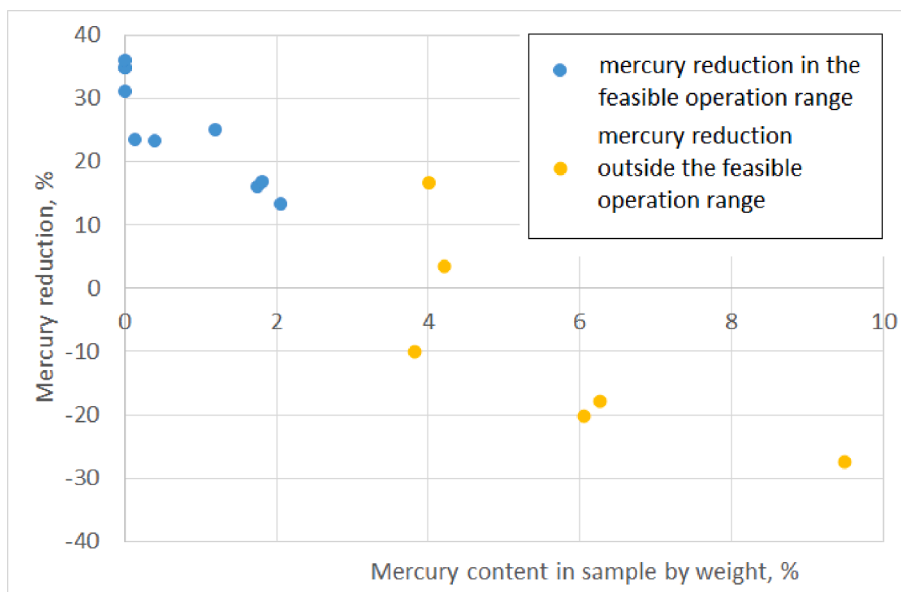


Fig. 8. Mercury reduction as a function of sample preload.

measurement revealed larger mercury concentration downstream of MC. Mercury reduction computed with eq. (7) was equal to -10 %. This shows that there is desorption of mercury from the sample. Desorption is a result of performing the preloading procedure at a very high mercury concentration. One have to keep in mind that at normal operating conditions it takes years for SPC material to absorb 1 %wt of mercury. As mentioned in section 2.1 preparing samples containing mercury was made using thousand times higher mercury concentration and thus shortening the procedure. Therefore, it is possible that part of mercury particles might be only attached to the SPC surface but not chemically bonded in the active carbon sorbent. As a result, these molecules may be detached from the SPC into the gas. An important information is that even for 10 years of operation SPC material will not achieve such high concentration of mercury.

The final tested parameter was the gas velocity, whose influence was tested for both mercury-free and preloaded samples (Fig. 9). One can see that upon increasing the velocity, mercury reduction decreased linearly due to a shorter contact time between gas and the SPC material. This trend is visible for both the mercury-free SPC, as well as the preloaded one. Additionally, the tests showed that this effect was stronger in the

preloaded material. The mercury reduction uncertainty comes from the uncertainty of mercury concentration itself (see eq. 3) and the uncertainty of the correction factor (see eq. 6). Using the law of error propagation and assuming independent variables:

$$s_{Hg} = \sqrt{\left(\frac{d\varepsilon}{dC_{in}}\right)^2 s_{C_{in}}^2 + \left(\frac{d\varepsilon}{dC_{out}}\right)^2 s_{C_{out}}^2 + \left(\frac{d\varepsilon}{df}\right)^2 s_f^2} \tag{8}$$

where  $s$  is the uncertainty of mercury reduction,  $f$  is the conversion factor (1/1.63). Solving eq. (8) for laboratory installation yields reduction uncertainty between 0.24 and 1.84 % depending on the measurement. Higher uncertainties are for cases with higher mercury reduction.

### 3.2. Industrial scale experiment

Before the measurements were taken the rig was conditioned for two months. Next, a set of six clean SPC modules were mounted on the rig, and the rig was further conditioned for another month. To imitate the actual operation of the SPC a spraying system is mounted in the top of the column. There the SPC material is washed twice a day to clean modules from any ash particles or other contaminations that can adhere

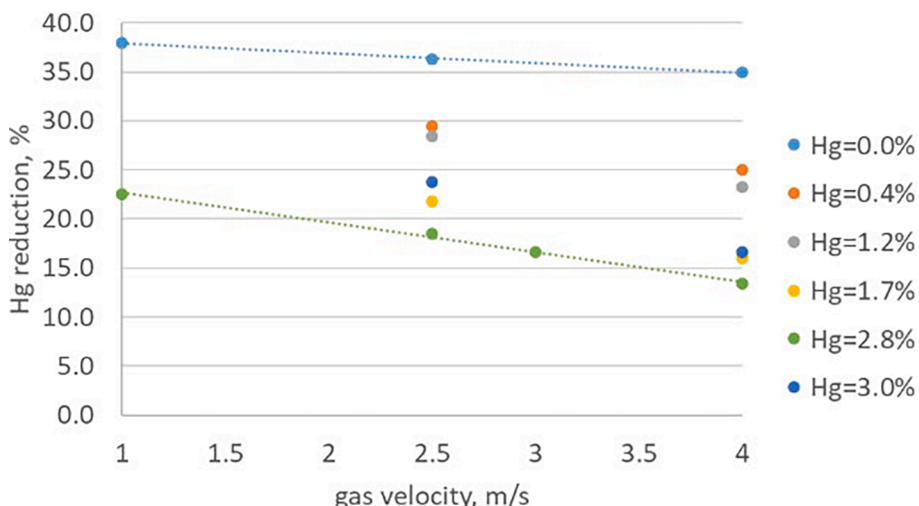


Fig. 9. SPC reduction potential versus gas velocity.

to the SPC. Measurements of mercury content were taken with the use of the Gaset continuous mercury measurement system. Gaset uses Cold Vapor Atomic Fluorescence to measure both total and elemental mercury. The analyzer is capable of accurately measuring a wide range of mercury concentrations even below  $1 \mu\text{g}/\text{m}^3$  with an uncertainty of about 4 %. Different measurement devices allowed for continuous measurement without any concentration oscillations. Unfortunately, due to the size of the Gaset system, it was not possible to use it for the laboratory experiment. The sample measurement of the mercury concentration on a test rig versus time is given in Fig. 10. The major difference between laboratory tests and operation on actual flue gas is the strong variation of mercury concentration at the inlet to installation. This variation is caused by different composition of fuel that is combusted in a power plant so it is a typical standard working condition of the power plant. For the industrial scale, experiment measurements were carried out for six days.

There the inlet concentration varied between about 10 and  $22 \mu\text{g}/\text{m}^3$ . Outlet concentration was between 2 and  $7 \mu\text{g}/\text{m}^3$ . The mercury reduction for this period varied between 52 and 86 % while the average value for the entire measurement period was equal to 71 %. This indicated that on average each SPC module reduces mercury content between 11.5 and 28 % with an average of 18.65 %. This is lower than the value foreseen in the laboratory tests by about 22 %. This can be explained by the fact that flue gas contains dust that can also attach to the material. Another reason for the differences between the lab and industrial installations is the presence of sulfur dioxide in the latter. This species undergoes catalytical oxidization to  $\text{SO}_3$  at the surface of SPC (as explained in section 2) blocking the access to the sorbent present in the material, which is not available for mercury adsorption. The  $\text{SO}_2$  concentration during the measurements varied between 140 and  $250 \text{ mg}/\text{Nm}^3$  at 6 %  $\text{O}_2$ . At the outlet from the installation, the concentration was in the range of 26–74  $\text{mg}/\text{Nm}^3$  at 6 %  $\text{O}_2$ . For the industrial installation, the mercury reduction uncertainty comes only from concentration measurement uncertainty as all measurements are integrated with the Gaset device. Therefore the law of error propagation gives:

$$s_{Hg} = \sqrt{\left(\frac{d\varepsilon}{dC_{in}}\right)^2 s_{C_{in}}^2 + \left(\frac{d\varepsilon}{dC_{out}}\right)^2 s_{C_{out}}^2} \quad (9)$$

Solving eq. (9) for industrial installation yields reduction uncertainty between 0.57 and 0.98 % depending on the measurement. Higher uncertainties are, like for laboratory tests, for cases with higher mercury reduction.

#### 4. Numerical modeling

Results from the laboratory tests were used as input to the numerical

model. There a percentage mercury reduction for one layer of the SPC module as a function of velocity was given by.

$$\varepsilon_{bv} = 0.5015v^2 - 6.7202v + 41.494 \quad (10)$$

which corresponds to the conditioned module i.e. containing minimal mercury amount. Additionally, a correction factor accounting for gas temperature was defined as.

$$C_T = -0.0012T + 1.3889 \quad (11)$$

For a CFD simulation, it was necessary to define a negative source of mercury applied to every cell located in the SPC reduction zone. The such source was defined as.

$$dm_{Hg,c} = -\frac{1}{V} my_{Hg} \left[ 1 - \left( \frac{100 - \varepsilon_{bv} C_T}{100} \right)^{L/L_c} \right] \quad (12)$$

where  $v$  is gas velocity, m/s,  $T$  is a gas temperature, K,  $V$  is a cell volume,  $\text{m}^3$ ,  $y_{Hg}$  is the mass fraction of mercury in a cell,  $L$  is the length of an SPC module (0.4 m) and  $L_c$  is a length of a cell in a flow direction of a gas, m. A such source was defined in every zone with a polymer module (see Fig. 11). There, depending on gas velocity and temperature mercury is removed.

The numerical model encompassed an inlet gas duct, a mercury adsorption chamber where 6 layers of SPC material are located and the outlet channel with a fan (Fig. 11). To simplify the model an actual fan was replaced by a pressure jump to cover the fan behavior. The numerical mesh was composed of almost 1 million hexahedral elements with average quality of 0.96 while the minimal was 0.74. The maximum aspect ratio for the mesh was less than 5. The flow was simulated using a steady state solver with a  $k-\varepsilon$  turbulence model and energy equation enabled. To enable an analysis of mercury a species-transport model was used. The density of a mixture was defined as for ideal-gas and specific heat for mixing law. Other gas properties were assumed constant which is a viable assumption since the temperature varies by about 2 K and the change in mass fractions in the gas is very small since only mercury is removed from the gas. Mass flow with 1.574 kg/s, 5 % turbulent intensity, and temperature of 341 K was used at the inlet of the model. Mercury mass fraction was defined as  $7.3\text{e-}9$  which corresponds to the typical mercury content in the flue gas. A pressure outlet with  $-100$  gauge pressure was set at the outflow from installation. The simulation was run with SIMPLE pressure-velocity coupling and spatial discretization set to second-order. SPC material was modeled as a porous zone with a  $y$ -direction pressure drop set as a function of velocity taken for the actual SPC module. Resistances in  $x$ - and  $z$ -directions were set thousand times higher to model the behavior of actual channels created by layers of SPC material. Computations were carried out in ANSYS/Fluent 15.7.

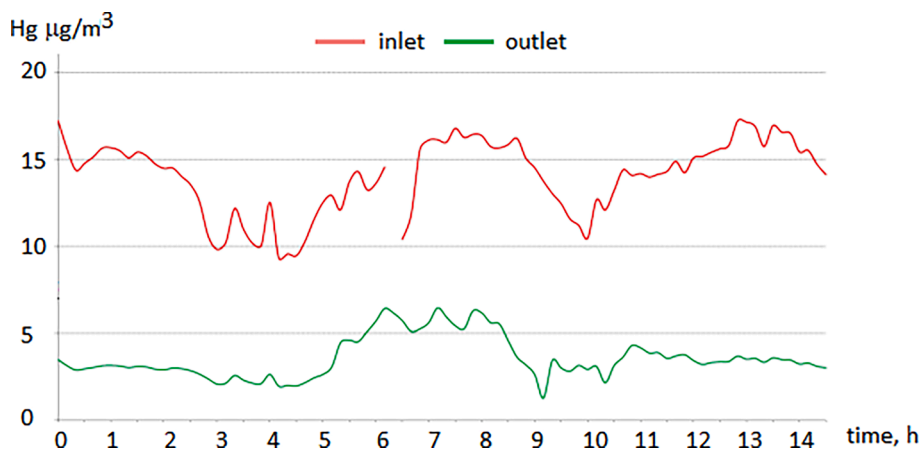


Fig. 10. Industrial scale test rig measurements.



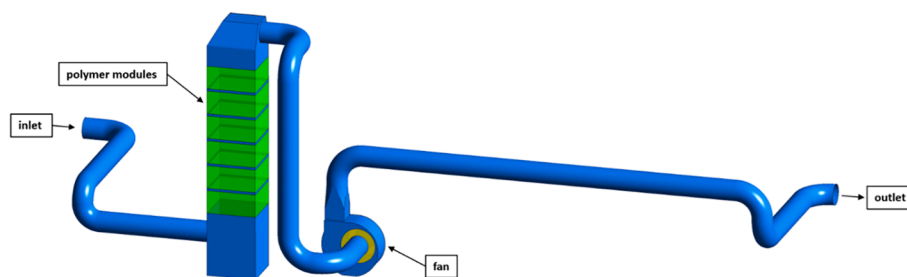


Fig. 11. Industrial scale test rig - geometry.

The industrial scale rig is designed so the average velocity in the adsorption chamber matches the actual velocity in the wet FGD system (see velocity field in Fig. 12). There the velocity should be within a range of 3.5 and 4 m/s. Simulation results have shown that the average velocity equals 3.7 m/s while the minimal is 3.4 and the maximal 3.8 m/s. This guarantees effective work of SPC material. The only significant difference in velocity field can be seen at the inlet to the first SPC layer. Their velocity variation was higher – between 3.4 and 4.4 m/s.

Analyzing Fig. 13 one can see that mercury concentration does not change until reaching the SPC section. Then, the mercury concentration is gradually reduced. The reduction (computed using eq. 3) is evaluated for every SPC layer and varies between 22 and 24 % (see Table 1), which is in accordance with results from the laboratory setup. This gives a total reduction of 78.7 %. The reduction resulting from the numerical model was higher than the measured one by about 19 %.

## 5. Results and discussion

It is important to note the behavior of the SPC material in laboratory tests when the mercury concentration in the SPC material exceeds 4 %. In this case, for some samples, the mercury concentration downstream is higher than upstream. This can be attributed to the desorption of mercury contained in the sample. However, one must keep in mind two things. The first is that the preloading of mercury to modules was carried out in different methods than those used in real scenarios – the mercury concentration in the preloading chamber was about 1000-times higher than the gas used in measurements. The second aspect is that the mercury loading time was on the order of hours, while in real cases, it would be years. Those two combined factors mean that it is possible that some of the mercury molecules using this test procedure was attached to the SPC surface by sorption but were not chemically bonded. As a result,

these molecules may be desorbed from the SPC into the gas. This phenomenon was confirmed by the results of the measurement. The experiments where the samples contained around 4 % mercury, show significant changes in their adsorption ability (Fig. 8). Two results showed a reduction (17 % and 4 %), while the third showed an almost 10 % higher mercury content in the gas. In actual operation, this would not happen because when the chemical equilibrium between the gas and SPC is achieved, no more mercury is captured. This observation is, therefore, an artifact of the test procedure, as indicated by the orange data points in Fig. 8. Besides, as mentioned earlier, the mercury loading in an actual power plant will typically be much lower than 4 %.

The test results were used to predict the behavior of a real system over 7 years of operation (see Fig. 14). Depending on the desired reduction level, several layers of these boxes are used. For the case at hand, an industrial installation would consist of 6 layers of the SPC. To obtain the reduction level and mercury content in the SPC over time, the blue points in Fig. 8 were approximated using the function.

$$\varepsilon = -1.647 \ln(C_{SPC}) + 19.295 \quad (11)$$

At the initial time, the average reduction using the SPC not containing mercury was 34.3 %. The mercury content by weight in SPC was calculated by assuming a constant mercury reduction within a given time interval, which was assumed to be one week. This time step is sufficiently small that it does not affect the results. An average inlet mercury concentration of  $12 \mu\text{g}/\text{Nm}^3$  and a velocity of 4 m/s were assumed in this simulation, and the results are shown in Fig. 14. The dashed line indicates the reduction potential of 6 layers of the SPC material. Initially, for modules without mercury, the Hg reduction exceeded 90 %. Within only a few weeks of operation in the first year, it dropped to about 80 %. This is a result of the initial performance drop visible in Fig. 5. After 7 years, the reduction potential decreased to 70 %.

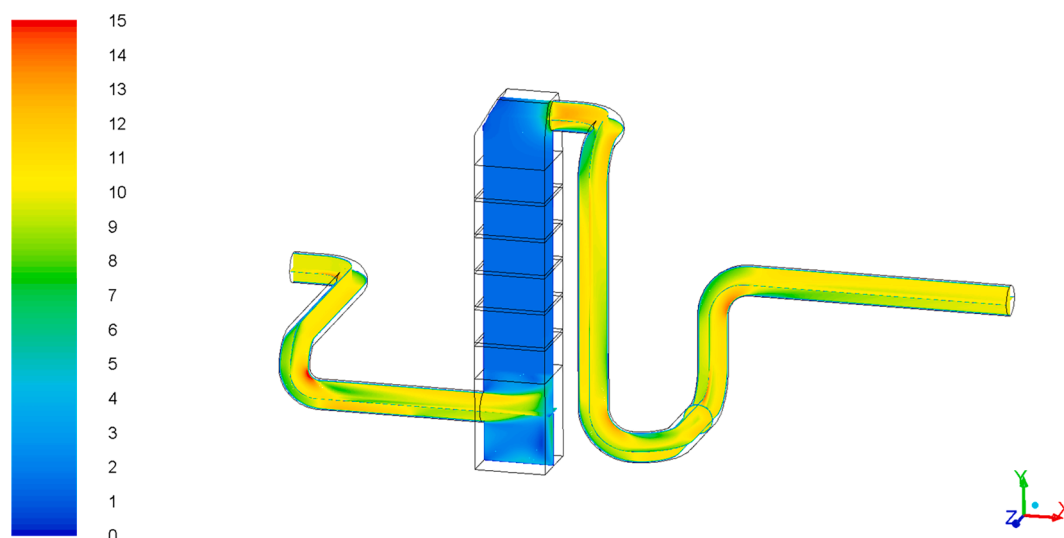


Fig. 12. Industrial scale test rig - velocity magnitude, m/s.

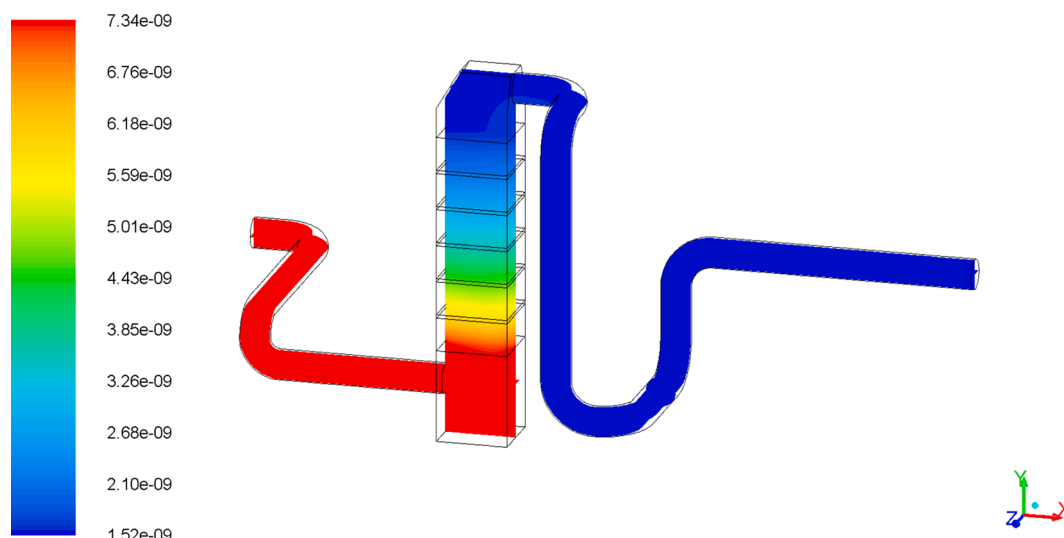


Fig. 13. Industrial scale test rig – a mass fraction of mercury.

Table 1

Mercury reduction for the industrial test rig.

Location	inlet	layer 1	layer 2	layer 3	layer 4	layer 5	layer 6
mass fraction	7.32e-9	5.59e-9	4.33e-9	3.35e-9	2.59e-9	2.00e-9	1.56e-9
reduction, %		24	23	23	23	23	22

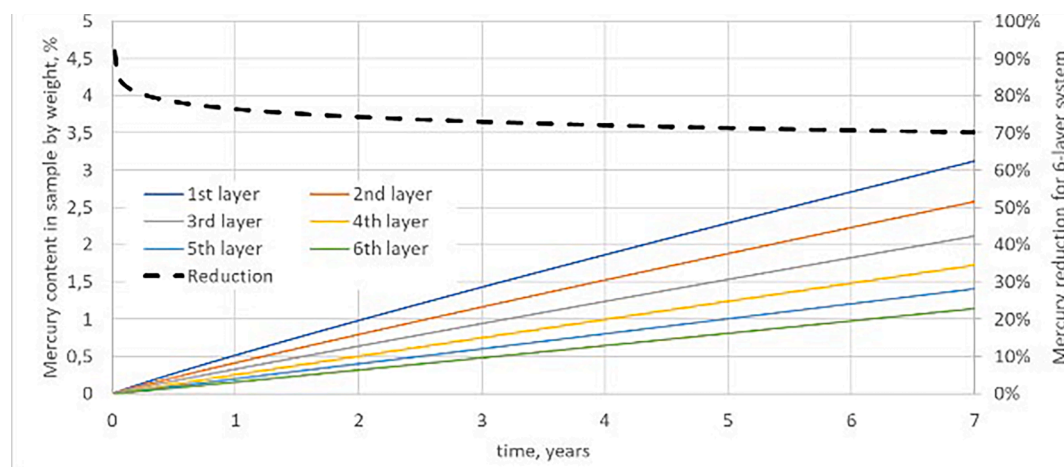


Fig. 14. Predicted reduction potential for long-term operation under real conditions.

The solid lines represent the mercury content in the SPC material within a given layer. The bottom layers are in contact with the highest mercury concentration in gas and thus, after 7 years, their mercury content increases to about 3 wt%. After the same time, the uppermost layer contained only 1.25 wt% mercury.

To get a more uniform mercury content and decrease the mechanical wear of the material, the manufacturer recommends reversing the SPC layers in the middle of its operation. Then, the highest mercury concentration is 2.5 %, while the lowest one is 1.7 %. Regardless of the situation, after 7 years of operation, there is no risk of reaching a reduction potential of zero. One has to keep in mind that as the concentration of mercury in the SPC material increases, its reduction potential decreases. This was shown by an experiment on an industrial installation. There SPC material operating on flue gas containing dust particles and after two months of conditioning showed performance lower by about 20 % than laboratory experiments and the CFD model.

This discrepancy originates from two sources. First is a measurement uncertainty that is in the range of 7 %. This is a combined uncertainty of a mercury analyzer itself, location of the probe and temperature measurement. The latter comes from the dust present in the flue gas that can stick to sorbent and reduce its active surface. Therefore, a correction coefficient was proposed to the numerical model when a system working on real flue gas is considered. This is an interesting feature as it can be beneficial to locate the SPC installation downstream to de-dusting installation as there the content of flying ash is minimal. The decreasing performance with increasing velocity indicates that it would be beneficial to reduce the gas velocity as much as possible. An additional benefit from velocity reduction would be a smaller pressure drop in the system. This has to be considered, as for already existing systems, any additional pressure drop can make it necessary to replace the exhaust gas fan. Additionally, this would require the use of more SPC boxes per layer, but at the same time, fewer layers are needed. Thus,

manipulating the velocity allows for more flexibility in installation design. Adjusting the flue gas velocity may also influence the CAPEX of the system.

## 6. Conclusions

This study has shown the capabilities of an SPC material to reduce the mercury concentration in flue gases generated by coal-fired power plants. The influence of the most important parameters on the reduction level was tested on a laboratory scale rig. The results showed that neither humidity nor temperature has a significant impact on the reduction level. Two of the most important factors influencing the SPC performance are velocity and mercury content in the material. With an increased velocity, the mercury reduction capability decreased because of the shorter contact time. Also, increasing the concentration of mercury inside the SPC decreased the capability of the material to chemically bind to mercury. To predict the behavior of the SPC membranes, a detailed analysis should be carried out to determine the required number of SPC layers and the SPC material lifespan.

The results of laboratory tests were used to develop a numerical model. The mercury removal model was used in the CFD model of an industrial installation to foresee mercury reduction for actual flue gas. The difference in mercury reduction from the CFD model and measurements was about 20 %. This significant difference comes from dust present in the flue gas that sticks to SPC material in reality but is not modeled. For this reason, an actual installation requires a washing system that frequently cleans SPC material from dust attached to its surface. As opposed to the most popular mercury reduction technique, i.e., carbon injection, the reduction potential of SPC does not depend on the mercury concentration in the gas. Therefore, a hybrid system can provide an economical approach. There, SPC should be used as a base method to reduce the basic mercury load, while activated carbon should be used to fine-tune the output mercury concentration. This is particularly important when the inlet mercury concentration varies significantly due to changes in the mercury content in fuel. The application of active coal injection provides a chance to bring the concentration of mercury to the desired level, as a system based on SPC has no degrees of freedom to adjust to rapidly changing levels of mercury in the fuel. This study gives important insight into the performance of SPC materials with increasing mercury content to predict the long-term behavior of SPCs.

Ethics approval and consent to participate: not applicable.

Consent for publication: not applicable

Availability of data and materials: The datasets used and/or analyzed during the current study are available from the corresponding author upon reasonable request.

## Funding

This research was co-financed by the European Regional Development Fund within the framework of the Smart Growth Operational Programme Grant No. POIR.01.02.00–00-0198/16 and partially financed by the statutory funds of the Silesian University of Technology.

## CRediT authorship contribution statement

**Arkadiusz Ryfa:** Methodology, Writing – original draft, Writing – review & editing. **Robert Żmuda:** Funding acquisition. **Sergiusz Mandrela:** Validation. **Ryszard Bialecki:** Conceptualization, Writing – review & editing. **Wojciech Adamczyk:** . **Marcin Nowak:** Investigation. **Łukasz Lelek:** Project administration. **Dominika Bandota:** Investigation. **Marcin Pichura:** Investigation. **Joanna Płonka:** Resources. **Magdalena Wdowin:** Methodology, Validation.

## Declaration of Competing Interest

The authors declare that they have no known competing financial

interests or personal relationships that could have appeared to influence the work reported in this paper.

## Data availability

Data will be made available on request.

## References

- [1] Choi S, Lee S-S. Mercury adsorption characteristics of Cl-impregnated activated carbons in simulated flue gases. *Fuel* 2021;299:120822.
- [2] Commission Implementing Decision (EU) 2021/2326 of 30 November 2021 establishing best available techniques (BAT) conclusions, under Directive 2010/75/EU of the European Parliament and of the Council, for large combustion plants: <https://eur-lex.europa.eu/legal-content/EN/TXT/?uri=CELEX%3A32021D2326>, accessed on 02.06.2022.
- [3] Czarna D, Baran P, Kunecki P, Panek R, Żmuda R, Wdowin M. Synthetic zeolites as potential sorbents of mercury from wastewater occurring during wet FGD processes of flue gas. *J Cleaner Production* 2018;172:2636–45. <https://doi.org/10.1016/j.jclepro.2017.11.147>.
- [4] Dziok T, Grzywacz P, Bochenek P. Assessment of mercury emissions into the atmosphere from the combustion of hard coal in a home heating boiler. *Environ Sci Pollut Res* 2019;26:22254–63. <https://doi.org/10.1007/s11356-019-05432-3>.
- [5] Dziok T, Strugała A, Włodek A. Studies on mercury occurrence in inorganic constituents of Polish coking coals. *Environ Sci Pollut Res* 2019;26:8371–82. <https://doi.org/10.1007/s11356-018-1667-1>.
- [6] Gore's passive Hg and SO<sub>2</sub> removal system makes its European commercial debut at Chemnitz, Modern Power Systems, October 2018, pages 24–25.
- [7] Granite J, Pennline HW. *Mercury Control for Coal-Derived Gas Streams*, Edited by Evan J. Granite: Henry W. Pennline, and Constance Senior, Wiley; 2015.
- [8] Hylander LD, Sollenberg H, Westas H. A three-stage system to remove mercury and dioxins in flue gases. *Sci Total Environ* 2003;304:137–44. [https://doi.org/10.1016/S0048-9697\(02\)00563-6](https://doi.org/10.1016/S0048-9697(02)00563-6).
- [9] Johari K, Saman N, Song ST, Chin CS, Kong H, Mat H. Adsorption enhancement of elemental mercury by various surface modified coconut husk as eco-friendly low-cost adsorbents. *Int Biodeterior Biodegrad* 2016;109:45–52.
- [10] Lee EM, Clack HL. Powder Resistivity Inferred Differential Collection of Heterogeneous Coal Fly Ash and Powered Activated Carbon Admixtures Within a Cylindrical Electrostatic Precipitator. *Emiss Control Sci Technol* 2016;2:33–43. <https://doi.org/10.1007/s40825-015-0029-4>.
- [11] Legislation, standards, and methods for mercury emissions control, ISBN 978-92-9029-515-0, April 2012, IEA Clean Coal Centre, [https://www.usea.org/sites/default/files/042012\\_Legislation%2C%20standards%20and%20methods%20for%20mercury%20emission%20control\\_ccc195.pdf](https://www.usea.org/sites/default/files/042012_Legislation%2C%20standards%20and%20methods%20for%20mercury%20emission%20control_ccc195.pdf), accessed on 11.09.2020.
- [12] Li H, Huang G, Yang Q, Zhao J, Liu Z, Yang J. Numerical simulation of sorbent injection for mercury removal within an electrostatic precipitator: In-flight plus wall-bounded mechanism. *Fuel* 2022;309:122142.
- [13] Liu H, Ruan W, Zhang Z, Zhou Y, Shen F, Liu J, et al. Performance and mechanism of CuS-modified MWCNTs on mercury removal: Experimental and density functional theory study. *Fuel* 2022;309:122238.
- [14] Liu Z, Wang D, Peng B, Chai L, Liu H, Yang S, et al. Transport and transformation of mercury during wet flue gas cleaning process of nonferrous metal smelting. *Environ Sci Pollut Res* 2017;24(28):22494–502.
- [15] Liu W, Zhou Y, Hua Y, Peng B, Deng M, Yan N, et al. A sulfur-resistant CuS-modified active coke for mercury removal from municipal solid waste incineration flue gas. *Environ Sci Pollut Res* 2019;26(24):24831–9.
- [16] Lyu Q, Liu Y, Guan Yu, Liu X, Che D. DFT study on the mechanisms of mercury removal from natural gas over Se-modified activated carbon, *Fuel*, 324. Part B 2022;324:124658.
- [17] Lv M, Luo G, Zou R, Ji Q, Fang C, Wang Li, et al. Study on the elemental mercury removal performance of co-pyrolyzed Cl-loading activated carbon and the formation mechanism of C-Cl functional groups. *Fuel* 2022;322:124229.
- [18] Marczak M, Budzyń S, Szczurowski J, Kogut K, Burmistrz P. Active methods of mercury removal from flue gases. *Environ Sci Pollut Res* 2019;26(9):8383–92.
- [19] Omine N, Romero CE, Kikkawa H, Wu S, Eswaran S. Study of elemental mercury re-emission in a simulated wet scrubber. *Fuel* 2012;91(1):93–101.
- [20] Uaciquete DLE, Sakusabe K, Kato T, Okawa H, Sugawara K, Nonaka R, Uaciquete, Kosuke Sakusabe, Takahiro Kato, Hirokazu Okawa, Katsuyasu Sugawara, Risehiro Nonaka, Influence of unburned carbon on mercury chemical forms in fly ash produced from a coal-fired power plant. *Fuel* 2021;300:120802.
- [21] United States Environmental Protection Agency, <https://www.epa.gov/mats/regulatory-actions-final-mercury-and-air-toxics-standards-mats-power-plant>, accessed on 02.06.2022.
- [22] Wang Y, Li H, He Z, Zhang M, Guan J, Qian K, et al. Removal of elemental mercury from flue gas using the magnetic Fe-containing carbon prepared from the sludge flocculated with ferrous sulfate. *Environ Sci Pollut Res* 2020;27(24):30254–64.
- [23] Wdowin M, Wiatros-Motyka MM, Panek R, Stevens LA, Franus W, Snape CE. Experimental study of mercury removal from exhaust gases. *Fuel* 2014;128:451–7. <https://doi.org/10.1016/j.fuel.2014.03.041>.
- [24] Wei J, He P, Jiang Wu, Chen N, Tianhong Xu, Shi E, et al. High-efficiency adsorption of elemental mercury from flue gas by K-intercalated 1T&2H MoS<sub>2</sub>. *Fuel* 2022;311. <https://doi.org/10.1016/j.fuel.2021.122615>.

- [25] WHO information on Mercury <https://www.who.int/news-room/fact-sheets/detail/mercury-and-health>, accessed on 11.09.2020.
- [26] Wilcox J, Rupp E, Ying SC, Lim D-H, Negreira AS, Kirchofer A, et al. Mercury adsorption, and oxidation in coal combustion and gasification processes. *Int J Coal Geology* 2012;90-91:4-20.
- [27] Yan R, Liang DT, Tay JH. Control of mercury vapor emissions from combustion flue gas. *Environ Sci & Pollut Res* 2003;10(6):399-407.
- [28] Yan R, Liang DT, Tsen L, Wong YP, Lee YK. Bench-scale experimental evaluation of carbon performance on mercury vapour adsorption. *Fuel* 2004;83:2401-9. <https://doi.org/10.1016/j.fuel.2004.06.031>.
- [29] Yang H, Xu Z, Fan M, Bland AE, Judkins RR. Adsorbents for capturing mercury in coal-fired boiler flue gas. *J Hazardous Materials* 2007;146(1-2):1-11.
- [30] Yang J, Shi N, Yan B, Wang T, Pan W-P. Removal of elementary mercury by solid sorbents at different temperatures: Variation of the desorption activation energy through thermal desorption analysis. *Fuel* 2022;307:121889.
- [31] Zhang Y, Duan W, Liu Z, Cao Y. Effects of modified fly ash on mercury adsorption ability in an entrained-flow reactor. *Fuel* 2014;128:274-80. <https://doi.org/10.1016/j.fuel.2014.03.009>.
- [32] Zhao S, Luo H, Ma A, Sun Z, Zheng R. Experimental study on mercury removal from coal-fired flue gas by sulfur modified biomass coke with mechanochemical method. *Fuel* 2022;309:122201.
- [33] Zhou Q, Duan Y-F, Hong Y-G, Zhu C, She M, Zhang J, et al. Experimental and kinetic studies of gas-phase mercury adsorption by raw and bromine modified activated carbon. *Fuel Process Technol* 2015;134:325-32. <https://doi.org/10.1016/j.fuproc.2014.12.052>.